

Received: 2019.04.13
Accepted: 2019.06.17
Published: 2019.10.23

Effect and Mechanism of the Bruton Tyrosine Kinase (Btk) Inhibitor Ibrutinib on Rat Model of Diabetic Foot Ulcers

Authors' Contribution:
Study Design A
Data Collection B
Statistical Analysis C
Data Interpretation D
Manuscript Preparation E
Literature Search F
Funds Collection G

CG 1 **Xuedong Yang**
BE 1 **Zhenhao Cao**
DF 2 **Peigang Wu**
AE 1 **Zhong Li**

1 Department of Hand and Foot Orthopedic Surgery, Weifang People's Hospital, Weifang, Shandong, P.R. China
2 Weifang Medical University, Weifang, Shandong, P.R. China

Corresponding Author: Zhong Li, e-mail: hw50360nu707@126.com
Source of support: Departmental sources

Background: Diabetes causes damage to the soft tissue and bone structure of the foot, referred to as "diabetic foot". Ibrutinib is a Bruton tyrosine kinase (Btk) inhibitor, and the role and mechanism of ibrutinib on the diabetic foot have not been elucidated.





Material/Methods: Male Wister rats were randomly divided into 3 groups: control group, model group, and ibrutinib group. After 14 days, the ulcer wound size of each group was measured, and the ulcer healing rate was calculated. The level of inflammatory factors interleukin (IL)-1 β , tumor necrosis factor (TNF)- α , and IL-6 was detected by enzyme-linked immunosorbent assay (ELISA). Real-time polymerase chain reaction (PCR) was used to analyze the changes of Toll-like receptor 2 (TLR2) and TLR4. The expression of vascular endothelial growth factor (VEGF) and the RAGE (receptor for advanced glycation end product/NF- κ B (nuclear factor-kappa B) pathway was detected by western blot.

Results: Blood glucose, blood lipids, serum creatinine, and urea nitrogen (BUN) levels were increased in the model group, together with increased levels of IL-1 β , TNF- α , IL-6, as well as TLR2 and TLR4 expression, and there were significant differences compared with the control group ($P < 0.05$). Meanwhile, the model group showed decreased VEGF expression and increased expression of RAGE and NF- κ B. However, ibrutinib reduced blood sugar, blood lipids, creatinine, and urea nitrogen levels, inhibited the secretion of inflammatory factors, promoted ulcer healing, improved ulcer healing rate, decreased the expression of TLR2, TLR4, RAGE, and NF- κ B, and increased VEGF expression; there were significant differences in the ibrutinib group compared with the model group ($P < 0.05$).

Conclusions: The Btk inhibitor ibrutinib can upregulate VEGF expression, inhibit the expression of TLRs, inhibit the secretion of inflammatory factors, and promote the healing of diabetic foot ulcer possibly by regulating the RAGE/NF- κ B pathway.

MeSH Keywords: **Inflammation • Rage • Vascular Endothelial Growth Factor A**

Full-text PDF: <https://www.medscimonit.com/abstract/index/idArt/916950>

 2542  2  5  25



Background

Diabetes is a common and frequent metabolic disease, and its incidence is increasing. There are nearly 300 million people with diabetes in the world with around 100 million diabetic patients in China [1,2]. Due to long-term hyperglycemia, diabetes can cause chronic diseases of various tissues and organs. Among these diseases is peripheral neuropathy caused by diabetes, combined with peripheral vascular disease, which causes excessive mechanical stress leading to the destruction of soft tissue and bone structure of the foot, called diabetic foot [3,4]. Diabetic foot is a serious complication of diabetes, a chronic progressive disease caused by vascular occlusive disease, leading to complications such as ischemia, peripheral neuropathy, and infection [5,6]. At least 25% of diabetic patients are likely to develop diabetic foot, and 85% of diabetic foot ulcers can eventually lead to amputation [7,8]. Epidemiological studies have reported that due to ischemia caused by diabetic nephropathy or peripheral vascular disease, diabetic distal limb neuropathy might occur, and then develops into diabetic foot [9].

Glucose and lipid metabolism disorders, inflammation, oxidative stress (OS), and apoptosis are important factors in the occurrence and development of diabetic foot [10]. The quality of life of patients with diabetic foot is seriously affected, and most of them are unable to work normally, causing enormous economic pressure and mental burden on patients, their families, and society [11]. The current treatment of diabetic foot is mainly symptomatic treatment, including debridement, treatment with appropriate antibiotics, and promotion of healing [12,13]. However, the current treatment for diabetic foot is not effective, and the patients' prognosis has not been significantly improved [14]. Btk (Bruton tyrosine kinase) belongs to Bruton tyrosine kinase family and is a tyrosine protein kinase in the cytoplasm. It can phosphorylate the corresponding substrate through recognizing the protein tyrosine residues. Sustained activation of Btk can lead to chronic inflammation and autoimmune disease [15]. Ibrutinib is a Btk inhibitor and is a novel immunomodulator that has been shown to play an important role in the treatment of diabetic nephropathy [16]. However, the role and mechanism of ibrutinib on diabetic foot has not been elucidated.

Material and Methods

Experimental animals

Healthy male Wister rats, 3 months old, SPF grade, body weight (250 ± 30 g), were purchased from the experimental animal center of Weifang Medical university and fed in a SPF animal experiment center. Feeding conditions included the temperature of $21\pm 1^\circ\text{C}$, relative humidity of 50% to 70%, and a 12/day cycle every 12 hours.

Main reagents and instruments

Ibrutinib and STZ were purchased from Sigma (USA). TRIzol reagent was purchased from Invitrogen (USA). The serum creatinine (Scr) test kit was purchased from Roche. PVDF membranes were purchased from Pall Life Sciences, EDTA were purchased from Hyclone (USA), RNA extraction kit and reverse transcription kit were purchased from Invitrogen. The western blot related chemical reagents were purchased from Shanghai Biyuntian Biotechnology Co., Ltd. Electrochemiluminescence (ECL) reagents were purchased from Amersham Biosciences. Anti-VEGF (vascular endothelial growth factor)/RAGE (receptor for advanced glycation end product/NF- κ B (nuclear factor-kappa B) were bought from Abcam, and rabbit anti-human SOX9 monoclonal antibody, and goat anti-rabbit horseradish peroxidase (HRP) labeled IgG secondary antibody were purchased from Cell Signaling, USA. The RNA extraction kit and the reverse transcription kit were purchased from Axygen, USA. The interleukin (IL)-1 β , tumor necrosis factor (TNF)- α , IL-6, and IL-10 ELISA test kits were purchased from R&D (USA). The rat special urea nitrogen detection reagent was purchased from Beijing Furui Bioengineering Co., Ltd. The Labsystem Version 1.3.1 microplate reader was purchased from Bio-rad Corporation of the United States. The PE Gene Amp PCR System 2400 DNA Amplifier was purchased from PE Corporation of the United States. The ACCU-CHEK electronic blood glucose meter was purchased from the American Advantage company. The AU5800 automatic biochemical analyzer was purchased from Beckman, Germany. Urine sugar test paper was purchased from Zhujiang Biochemical Reagent Company. Other commonly used reagents were purchased from Shanghai Shenggong Biological Co., Ltd.

DF model preparation

After 1 week of adaptive feeding of rats, the rat model preparation was performed. However, before the model preparation, rats were fasting for 12 hours, but had access to water. The tail veins of the model rats were injected with 0.5% streptozotocin (STZ) prepared in sterile citrate-sodium citrate buffer at a dose of 50 mg/kg, and the control group was injected with the same amount of citric acid-sodium citrate buffer. After 2 weeks, blood sugar, urine sugar, and urine volume were measured. The model was successfully established if the blood sugar was higher than 16.7 mmol/L, the urine sugar was below ++, and the urine volume was at least doubled. After successful preparation, the rats were anesthetized with 10% sodium pentobarbital. A wound of about 4×4 cm² was prepared in the skin thickness of the back of the rat, and the wound depth reached the fascia, and the diabetic foot model was thus prepared. The same size wounds were prepared in the same part of the control group and the ibrutinib group [17].

Table 1. Primer sequences for real-time polymerase chain reaction.

Gene	Forward 5'–3'	Reverse 5'–3'
GADPH	AGTGCCAGCCTCGTCTCATAG	CGTTGAACTTGCCGTGGGTAG
TLR2	AGCATCTAAGGCTCACAATGG	GGCCTCTCGCACATTGTA
TLR4	TCATAGTAGACATCTAGCCTC	ACTTAGCTTCTTGACGGTAGG

GADPH – glyceraldehyde 3-phosphate dehydrogenase; TLR – toll-like receptor.

Grouping of experimental animals

Thirty experimental rats were randomly divided into 3 groups with n=10 in each group (control group, model group, and ibrutinib group), in which model rats received intraperitoneal injection of ibrutinib (2 µM) for a continuous 4 weeks (once/daily) [17].

Specimen collection

After treatment, rat abdominal aorta blood samples were collected in a vacuum biochemical tube by vacuum storage method, and allowed to stand at room temperature for 30 minutes followed by centrifugation at 4°C at 3600 rpm for 10 minutes to collect the supernatant, which was stored in a refrigerator at –20°C for later use. The rats in each group were sacrificed and the wound tissue of the skin was stored in a refrigerator at –80°C for use.

Detection of renal function indicators

Blood glucose, blood lipids, Scr, and BUN changes were analyzed using an automated biochemical analyzer.

Enzyme-linked immunosorbent assay (ELISA) analysis of IL-1β, TNF-α, and IL-6 level

The serum was collected and the level of interleukin (IL)-1β, tumor necrosis factor (TNF)-α, and IL-6 were detected by enzyme-linked immunosorbent assay (ELISA) according to kit instructions. The main operation steps include: taking out a 96-well plate and adding 50 µL of the sequentially diluted standard to the corresponding reaction well to prepare a standard curve. 50 µL of the enzyme labeling reagent was added to each well except for the blank well. Mix gently by shaking and incubate for 30 minutes at 37°C. Wash the plate 5 times. Add 50 µL of the developer A to each well, then add 50 µL of the developer B, gently shake and mix, and develop at 37°C for 10 minutes in the dark. The enzyme plate was taken out, and 50 µL of the stop solution was added to each well to terminate the reaction (in this case, the blue color turned yellow). The blank value was zeroed, and the optical density value (OD value) of each well was measured by a microplate reader at a

wavelength of 450 nm. The measurement should be carried out within 15 minutes after the addition of the stop solution. The linear regression equation of the standard curve is calculated according to the concentration of the standard product and the corresponding OD value, and the corresponding sample concentration is calculated on the regression equation according to the OD value of the sample.

Real-time polymerase chain reaction (PCR)

Under sterile conditions, the skin tissue of the back wounds of each group was isolated followed by extraction of total RNA using TRizol reagent and subsequent transcription into cDNA. Real-time polymerase chain reaction (PCR) was used to detect the expression of the target gene using the designed primers (Table 1). Reaction conditions: 52°C for 1 minute, 90°C for 30 seconds, 58°C for 50 seconds, 72°C for 35 seconds, for a total of 35 cycles. Fluorescence quantitative PCR reactor software was used to collect relevant data. According to the internal reference GAPDH, the standard cycle number (CT) of the standard was calculated, and the standard curve was drawn. The quantitative analysis was analyzed by 2^{-ΔΔCt} method.

Western blot analysis of VEGF, RAGE, and NF-κB protein expression

Total tissue protein from the back wound skin of each group was extracted: RIPA lysate containing protease inhibitor (150 mM NaCl, 1% NP-40, 0.1% SDS, 2 µg/mL aprotinin, 2 µg/mL leupeptin, 1 mM PMSF, 1.5 mM EDTA, 1 mM NaVanadate), lysate the cells on ice for 15 to 30 minutes, then 5 second sonication 4 times, centrifuge at 15°C for 10 minutes, and transfer the supernatant to a new Eppendorf (Ep) tube. The protein was quantified and stored at -20°C for western blot analysis. The isolated protein was separated on a 10% sodium dodecyl sulfate polyacrylamide gel electrophoresis (SDS-PAGE), transferred to a polyvinylidene difluoride (PVDF) membrane and blocked with 5% skim milk powder for 2 hours. Then, primary antibody against VEGF (1: 1000 dilution), RAGE (1: 1000) and NF-κB (1: 2000) was incubated with the membrane at 4°C, overnight. After washing with PBST, HRP-conjugated secondary antibody (1: 2000) was incubated with the membrane for 30 minutes at room temperature followed by PBST wash,

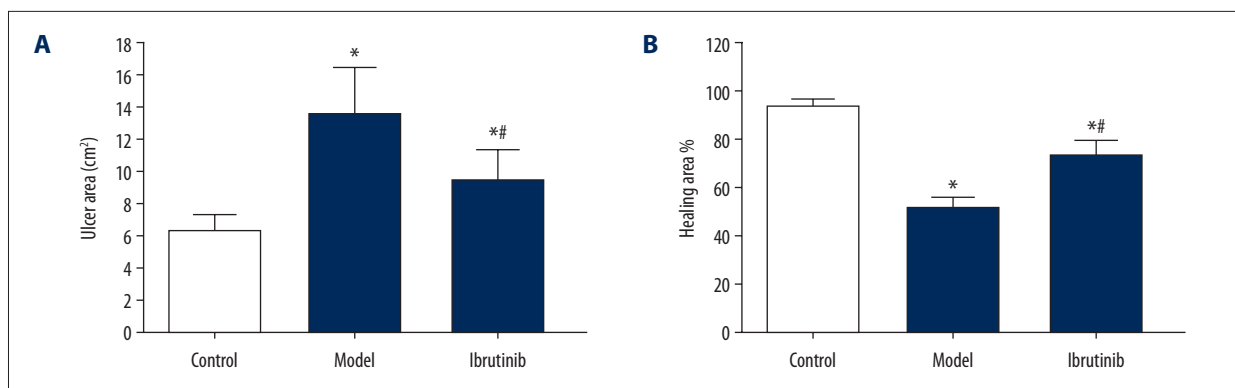


Figure 1. Effect of ibrutinib on ulcer size and healing rate in diabetic foot ulcer model. (A) Diabetic foot ulcer model changes the ulcer area; (B) diabetic foot ulcer model ulcer healing area. Compared with control group, * $P < 0.05$; compared with model group, # $P < 0.05$.

Table 2. Effects of Ibrutinib on blood glucose, blood lipids, creatinine and urea nitrogen in diabetic foot ulcer model.

Parameters	Control	Model	Ibrutinib
Weight (g)	421.4±22.7	251.9±26.8*	322.1±32.2*#
Blood glucose (mmol/L)	6.2±0.2	32.4±2.2	19.1±2.5*#
Scr (μmol/L)	91.6±12.5	571.7±41.8*	282±81.5*#
BUN (mmol/L)	6.8±0.6	14.7±1.3*	10.2±1.2*#
TC (mmol/L)	1.6±0.2	3.5±0.6*	2.2±0.6*#
TG (mmol/L)	0.6±0.1	1.7±0.3*	1.1±0.5*#

Scr – serum creatinine; BUN – blood urea nitrogen; TC – total cholesterol; TG – triglycerides. Compared with the control group, * $P < 0.05$; compared with the model group, # $P < 0.05$.

chemiluminescence for 1 minute, x-ray exposure imaging, observation results. X-film and strip density measurements were separately scanned using protein image processing system software and Quantity One software. The experiment was repeated 4 times.

Ulcer area measurement and healing rate analysis

The changes of ulcer area in each group were measured and the healing rate was calculated. Healing rate = healing area/original wound area × 100%; healing area is the difference between the original wound area and the unhealed wound area.

Statistical analysis

All data were expressed as mean ± standard deviation (SD) using SPSS 11.5 statistical software. Differences between groups were analyzed by analysis of variance (ANOVA), and the mean values of the 2 groups were compared using Student's *t*-test. The enumeration data was presented as % and compared by chi-square test. $P < 0.05$ indicated a statistical significance.

Results

Effect of ibrutinib on ulcer size and healing rate in diabetic foot model

The ulceration of diabetic foot rat ulcer model was small, and the healing rate was low. Compared with the control group, the difference was statistically significant ($P < 0.05$). The treatment of diabetic foot rat ulcer model with ibrutinib significantly reduced the ulcer area and improved the healing rate, with statistical differences compared with model group ($P < 0.05$) (Figure 1).

Effect of ibrutinib on blood sugar, blood lipid, Scr, and BUN

The levels of blood glucose, blood lipids, Scr, and BUN in the diabetic rat model of ulcer were significantly increased compared with those in control group ($P < 0.05$). Ibrutinib treatment significantly reduced the levels of blood sugar, blood lipids, Scr, and BUN level compared with the model group ($P < 0.05$) (Table 2).

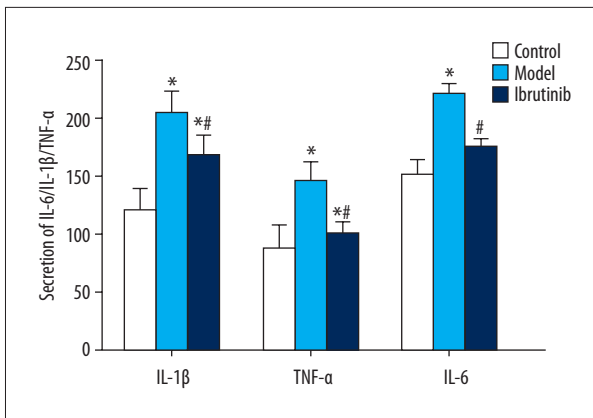


Figure 2. Effect of ibrutinib on inflammatory factors in diabetic rat model of ulcer. Compared with the control group, * $P < 0.05$; compared with the model group, # $P < 0.05$.

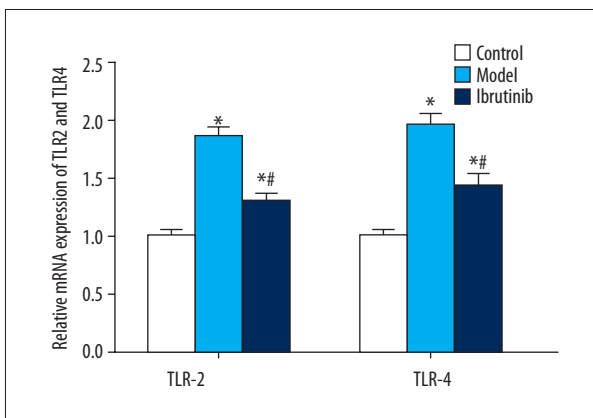


Figure 3. Effect of ibrutinib on the expression of TLR2 and TLR4 in diabetic rat model of ulcer. Compared with the control group, * $P < 0.05$; compared with the model group, # $P < 0.05$.

Effect of ibrutinib on inflammatory factors in diabetic foot ulcer rat model

The levels of inflammatory factors IL-1 β , TNF- α , and IL-6 were significantly increased in the diabetic rat model of ulceration compared with those in control group ($P < 0.05$). Ibrutinib treatment significantly decreased the secretion of IL-1 β , TNF- α , and IL-6 compared with model group ($P < 0.05$) (Figure 2).

Effect of ibrutinib on the expression of Toll-like receptors 2 (TLR2) and TLR4

Real-time PCR was used to detect the effect of ibrutinib on the expression of Toll-like receptors 2 (TLR2) and TLR4 in rat model of diabetic foot ulcer. The expression of TLR2 and TLR4 in ulcerated skin tissue was significantly increased in the diabetic foot ulcer rat model compared with those in the control group ($P < 0.05$). Ibrutinib decreased the expression of TLR2 and

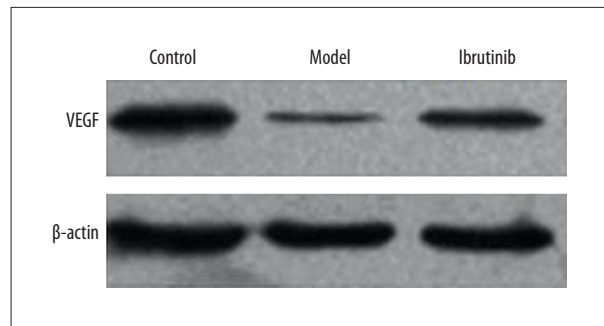


Figure 4. Effect of ibrutinib on vascular endothelial growth factor (VEGF) in a rat model of diabetic foot ulcer.

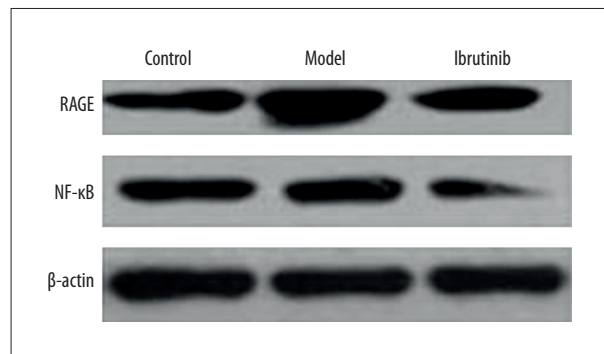


Figure 5. Effect of ibrutinib on RAGE/NF- κ B signaling pathway in diabetic rat model of ulcer.

TLR4 in ulcerated skin tissue with a statistical significance difference in the ibrutinib group compared with the model group ($P < 0.05$) (Figure 3).

Effect of ibrutinib on VEGF in a rat model of diabetic foot ulcer

The expression of VEGF was decreased in the diabetic rat model of ulceration, and ibrutinib promoted the expression of VEGF in the rat model of diabetic foot ulcer (Figure 4).

Effect of ibrutinib on RAGE/NF- κ B signaling pathway

The effect of ibrutinib on RAGE/NF- κ B signaling pathway in diabetic foot ulcer model was further analyzed. The results showed that the expression of RAGE and NF- κ B in the diabetic rat model of ulcer increased, while ibrutinib decreased the expression of RAGE and NF- κ B in the diabetic foot ulcer model (Figure 5).

Discussion

Diabetes can cause microvascular disease and hemodynamic disorder, leading to multiple organ damage. The foot is considered one of the target organs of multi-systemic diseases of diabetes,

and blood vessels and peripheral neuropathy can cause inflammation, infection, ulcer, food malformation, and even amputation in severe cases [18]. The treatment of diabetes and its complications imposes a huge economic burden on patients and world health institutions. Therefore, choosing effective treatment can reduce the incidence of diabetes and diabetic foot [19].

Btk phosphorylates protein tyrosine is a member of the non-receptor tyrosine protein kinase family, which plays a role in a variety of cell development processes [20]. Btk can regulate the differentiation, development, activation, proliferation, and apoptosis of B cells, and participate in the regulation of inflammation, bone cell development, and tumors [21]. The Btk selective small molecule inhibitor ibrutinib can inhibit the tyrosine kinase activity, cause oral irreversible inhibition of NF- κ B signaling pathway, and subsequent inhibition of the expression of inflammatory factors, and plays a role in the treatment of diabetic nephropathy [16,22]. Therefore, this study aimed to analyze the effect of ibrutinib on a rat model of diabetic foot ulcer. The results confirmed that ibrutinib can reduce blood sugar, blood lipids, Scr, and BUN levels, inhibit inflammatory factor secretion, promote ulcer healing, and improve ulcer healing rate in diabetic foot ulcer models. The data suggest that ibrutinib can inhibit the progression of inflammation in the rat model of diabetic foot ulcer, thereby controlling the blood sugar and lipid metabolism of diabetes, which then effectively alleviate the progression of ulcers.

TLRs are one of the pattern recognition receptors involved in innate immunity, a class of important protein molecules that link natural immunity with specific immunity. TLR2 and TLR4, as members of the TLRs family, play an important role

in inflammation, bacterial infection, and autoimmune diseases [23]. The regulation of VEGF expression can improve the microvascular lesions in diabetes, resulting in insufficient local blood perfusion, and thus regulates the progression of diabetic foot disease [24]. The RAGE/NF- κ B signaling pathway is an important inflammatory factor regulatory pathway, and its activation will lead to further deterioration of diabetic foot [25]. In the present study, we confirmed that ibrutinib can down-regulate the expression of TLR2 and TLR4 in diabetic rat model of ulcer, promote the expression of VEGF, and decrease the expression of RAGE and NF- κ B, suggesting that ibrutinib can downregulate the expression of VEGF and inhibit the expression of TLRs possibly by regulating RAGE/NF- κ B pathway. In turn, it inhibits the progression of inflammation and promotes ulcer healing. In further research, we will explore the efficacy and related mechanisms of ibrutinib in the treatment of patients with clinical diabetic foot ulcers and provide more theoretical basis for the clinical use of ibrutinib.

Conclusions

Btk inhibitor ibrutinib can upregulate the expression of VEGF and inhibit the expression of TLRs by regulating the RAGE/NF- κ B pathway, thereby inhibiting the secretion of inflammatory factors IL-1 β , TNF- α , and IL-6, and promoting the healing of diabetic foot. This study provides a reference for the selection of new drugs for clinical treatment of diabetic foot.

Conflict of interest

None.

References:

- Zhan X, Yan C, Chen Y et al: Celastrol antagonizes high glucose-evoked podocyte injury, inflammation and insulin resistance by restoring the HO-1-mediated autophagy pathway. *Mol Immunol*, 2018; 104: 61–68
- Du N, Xu Z, Gao M et al: Combination of ginsenoside Rg1 and astragaloside IV reduces oxidative stress and inhibits TGF- β 1/Smads signaling cascade on renal fibrosis in rats with diabetic nephropathy. *Drug Des Devel Ther*, 2018; 12: 3517–24
- Ugwu E, Adeleye O, Gezawa I et al: Burden of diabetic foot ulcer in Nigeria: Current evidence from the multicenter evaluation of diabetic foot ulcer in Nigeria. *World J Diabetes*, 2019; 10(3): 200–11
- Carabott M, Formosa C, Mizzi A et al: Thermographic characteristics of the diabetic foot with peripheral arterial disease using the angiosome concept. *Exp Clin Endocrinol Diabetes*, 2019 [Epub ahead of print]
- Denhez B, Rousseau M, Dancosst DA et al: Diabetes-induced DUSP4 reduction promotes podocyte dysfunction and progression of diabetic nephropathy. *Diabetes*, 2019; 68(5): 1026–39
- Abouhamda A, Alturkstani M, Jan Y: Lower sensitivity of ankle-brachial index measurements among people suffering with diabetes-associated vascular disorders: A systematic review. *SAGE Open Med*, 2019; 7: 2050312119835038
- Elmarsafi T, Anghel EL, Sinkin J et al: Risk factors associated with major lower extremity amputation after osseous diabetic Charcot reconstruction. *J Foot Ankle Surg*, 2019; 58(2): 295–300
- Mu S, Hua Q, Jia Y et al: Effect of negative-pressure wound therapy on the circulating number of peripheral endothelial progenitor cells in diabetic patients with mild to moderate degrees of ischaemic foot ulcer. *Vascular*, 2019; 27(4): 381–89
- Rastogi A, Bhansali A, Ramachandran S: Efficacy and safety of low-frequency, noncontact airborne ultrasound therapy (glybetac) for neuropathic diabetic Foot Ulcers: A randomized, double-blind, sham-control study. *Int J Low Extrem Wounds*, 2019; 18(1): 81–88
- Moon KC, Chung HY, Han SK et al: Possibility of injecting adipose-derived stromal vascular fraction cells to accelerate microcirculation in ischemic diabetic feet: A pilot study. *Int J Stem Cells*, 2019; 12(1): 107–13
- Wang T, Li X, Fan L et al: Negative pressure wound therapy promoted wound healing by suppressing inflammation via down-regulating MAPK-JNK signaling pathway in diabetic foot patients. *Diabetes Res Clin Pract*, 2019; 150: 81–89
- Francia P, Bellis A, Seghieri G et al: Continuous movement monitoring of daily living activities for prevention of diabetic foot ulcer: A review of literature. *Int J Prev Med*, 2019; 10: 22
- Lindholm E, Löndahl M, Fagher K et al: Strong association between vibration perception thresholds at low frequencies (4 and 8 Hz), neuropathic symptoms and diabetic foot ulcers. *PLoS One*, 2019; 14(2): e0212921
- Levy N, Gillibrand W: Management of diabetic foot ulcers in the community: An update. *Br J Community Nurs*, 2019; 24(Suppl.3): S14–19

15. Younes A, Sehn LH, Johnson P et al: Randomized phase III trial of ibrutinib and rituximab plus cyclophosphamide, doxorubicin, vincristine, and prednisone in non-germinal center B-cell diffuse large B-cell lymphoma. *J Clin Oncol*, 2019; 37(15): 1285–95
16. Fan Z, Wang Y, Xu X et al: Inhibitor of Bruton's tyrosine kinases, PCI-32765, decreases pro-inflammatory mediators' production in high glucose-induced macrophages. *Int Immunopharmacol*, 2018; 58: 145–53
17. Harrington BK, Wheeler E, Hornbuckle K et al: Modulation of immune checkpoint molecule expression in mantle cell lymphoma. *Leuk Lymphoma*, 2019 [Epub ahead of print]
18. Ning J, Zhao H, Chen B et al: Argon mitigates impaired wound healing process and enhances wound healing *in vitro* and *in vivo*. *Theranostics*, 2019; 9(2): 477–90
19. García-Álvarez Y, Lázaro-Martínez JL, Molines-Barroso RJ: Reflections on the effects of nitric oxide produced by a new dressing in the local management of diabetic foot ulcers. *Ann Transl Med*, 2018; 6(Suppl.2): 101–3
20. Islam S, Paek AL, Hammer M et al: Drug-induced aneuploidy and polyploidy is a mechanism of disease relapse in MYC/BCL2-addicted diffuse large B-cell lymphoma. *Oncotarget*, 2018; 9(89): 35875–90
21. Castillo JJ, Itchaki G, Paludo J et al: Ibrutinib for the treatment of Bing-Neel syndrome: A multicenter study. *Blood*, 2019; 133(4): 299–305
22. Kanagal-Shamanna R, Jain P, Patel KP et al: Targeted multigene deep sequencing of Bruton tyrosine kinase inhibitor-resistant chronic lymphocytic leukemia with disease progression and Richter transformation. *Cancer*, 2019; 125(4): 559–74
23. Liu D, Yang P, Gao M et al: NLRP3 activation induced by neutrophil extracellular traps sustains inflammatory response in the diabetic wound. *Clin Sci*, 2019; 133(4): 565–82
24. Zhu Y, Wang Y, Jia Y et al: Roxadustat promotes angiogenesis through HIF-1 α /VEGF/VEGFR2 signaling and accelerates cutaneous wound healing in diabetic rats. *Wound Repair Regen*, 2019; 27(4): 324–34
25. Massey N, Puttachary S, Mahadev-Bhat S et al: HMGB1-RAGE signaling plays a role in organic dust-induced microglial activation and neuroinflammation. *Toxicol Sci*, 2019; 169(2): 579–92